RJ10223 (A0110-039) October 30, 2001
Chemistry

IBM Research Report

The influence of resist components on image blur in a patterned positive-tone chemically amplified photoresist

Frances A. Houle, William D. Hinsberg, Martha I. Sanchez, John A. Hoffnagle
IBM Research Division
Almaden Research Center
650 Harry Road
San Jose, CA 95120

Research Division
Almaden - Austin - Beijing - Delhi - Haifa - India - T. J. Watson - Tokyo - Zurich

The influence of resist components on image blur in a patterned positive-tone chemically amplified photoresist

F. A. Houle, W. D. Hinsberg, M. I. Sanchez and J. A. Hoffnagle
IBM Almaden Research Center, 650 Harry Road, San Jose, CA 95120

Abstract

Post-exposure bake-induced blurring of the latent image in a chemically amplified photoresist may limit the extendability of this resist technology to printing of nanoscale features. It had been proposed that blurring is caused by thermally-assisted diffusion of photogenerated acid, however our experimental and kinetic modelling investigations of coupled reaction-diffusion in a resist system consisting of a photoacid generator in p-t-butyloxycarbonyloxystyrene (PTBOCST) has shown that the very high efficiency of acidolysis chemistry at the edge of an exposed region is actually responsible for blurring. Studies of the role of added base and the impact of photoacid generator size on blur support this view. These previous studies were performed with a 1-dimensional geometry. In order to test the relevance of the 1-D blurring model to pattern formation, we have carried out new investigations of blurring in dense line-space patterns using the same PTBOCST resist systems as in our earlier work. Resist films were imprinted with 866 nm and 192 nm pitch gratings generated by interferometric lithography using 257 nm light. The extent of deprotection over a range of doses and bake times at 85 C was measured by infrared spectroscopy, and compared to results of simulations of the bake process using the experimental aerial image and kinetics determined in the previous work. Experiment and predictions are in good agreement in all cases, indicating that the 1-dimensional kinetics are extendable to the 2-dimensional case. The simulations permit visualization of the relationship between the acid latent image and the developable image that forms in the polymer, enabling a deeper appreciation

of the influences of the resist components and of resist processing conditions on latent image transformations during post-exposure bake.

Introduction

The image formation process in chemically amplified resists determines the usefulness of this class of materials for printing patterns of nanoscale dimensions, whether the illumination source is light or charged particles.[1] Significant attention has been paid to the possibility that diffusion of resist components such as photogenerated acid will be sufficiently fast at normal post-exposure processing temperatures that an image on the sub-100 nm scale would be significantly blurred in many resist systems. A realistic assessment of this possibility requires that the chemistry and physics of image formation and transformation during resist processing be well characterized using quantitative techniques.[1,2]

As a first step toward understanding very complex fully formulated resist systems, which typically comprise copolymers, one or more photoacid generators, base, dissolution inhibitors and various inert additives designed to improve film-forming characteristics, we have investigated blurring in a model resist system using p-t-butyloxycarbonyloxystyrene (PTBOCST) homopolymer with a photoacid generator (PAG) and a base.[2-5] In those experiments, a thin, well-defined acidified layer was created using 193 nm light in the near-surface region of a PTBOCST film containing a PAG. This wavelength is strongly absorbed and completely decomposes all the PAG, thus avoiding the uncertainties in acid concentrations and interfacial structure and composition that can accompany the use of multi-layered films.[2] An additional benefit of the resulting high acid concentrations is that possible surface effects on diffusion resulting from contamination or polymer structure are minimized. The photogenerated acid catalyzes deprotection of the polymer at elevated temperatures during a post-exposure bake (PEB) step. This process is followed in real time using an infrared microscope, leading to

concentration vs time data that can be modelled using coupled reaction-diffusion chemical kinetics simulations. Using the deprotection kinetics measured independently, the simulations have been used to extract diffusion coefficients for acid [2] and to obtain a quantitative description for the role of an ionic base in controlling resist images.[3]

The diffusion process was found to be sensitive to the local environment in the polymer, as is to be expected because it involves migration of coupled protons and anions through a medium that is converting from non-polar to polar as deprotection proceeds. The size of the anion is important: t-butyl iodonium trifluoromethanesulfonic acid (TBI-T) migrates much more quickly than t-butyl iodonium perfluorobutanesulfonic acid (TBI-PFBS), but further increases in size of perfluorinated PAGs have little effect.[3,4] Addition of tetrabutylammonium hydroxide (TBAH) affects the deprotection rate by a combination of processes.[3] The kinetics are consistent with base association with the PAG during film casting, so that the initial acid latent image is proportionately reduced in local concentration through a pre-neutralization process. Any base remaining in unirradiated areas is available to trap diffusing acid.

The acid diffusion kinetics used in these investigations were assumed to be Fickian, that is, driven only by the local instantaneous concentration gradients. It has been proposed that free volume generated in the PTBOCST resist during deprotection because of the large density change involved would provide a strong transient enhancement of diffusion rates, dominating the transport process during post-exposure bake.[6-8] We have directly measured the amount of free volume formed, and have found it to be below our detection limit (1%), indicating that polymer relaxation is fast.[5] This result indicates that a simple Fickian description of the diffusion process

contains all the appropriate physics to describe the data we have collected to date, although it is certainly possible that refinement of the model may be necessary as our experiments become more detailed. Recently, the roles of transient diffusion[9] and free volume[10] have been reexamined, and it has been concluded that neither play a significant role in blurring printed images, in agreement with our previous work.[2,3]

Our experiments and simulations have allowed the following physical picture of blurring to emerge. Exposure causes acid to be formed in illuminated areas, with a gradient tailing vertically into the resist film due to attenuation in top-down illumination. Such a gradient would also be formed laterally when diffraction occurs at feature edges on a mask. The simulations show the acid profile to be quite stable during post-exposure bake, indicating that the blurring is due to the presence of the acid gradient at the edge of the exposed region, and the very long catalytic chain length of the acid-driven deprotection process.[2] Even very low concentrations of acid can lead to significant amounts of deprotection at long times. Thus, the blurring process has a significant chemical component not captured by simple diffusive models. This result does not mean that diffusion can never dominate blurring, indeed whenever the diffusion coefficient is very high, as found for TBI-T, or the local acid gradient is very steep, the diffusion rate can become competitive with the deprotection rate, and play a direct role in limiting feature size. Proximity in temperature to the T_g of the polymer, and use of weak rather than strong acids may also enhance diffusivity.[11]

It is possible to estimate the dimension range where acid diffusion would dominate image blur for a particular resist formulation using the reaction-diffusion kinetics determined in the

top-down experiments. The local extent of deprotection of a line-space array patterned resist film can be calculated as a function of pitch. Total blurring is measured by comparing the calculated linewidth to the nominal linewidth at the 80% deprotected level, where the resist is expected to be fully soluble.[12] The results of such an exercise for the TBI-PFBS/PTBOCST system are shown in Figure 1 for linewidths ranging from 21.3 to 340 nm. It can be seen that for this resist system the chemical component of blurring dominates imaging down to linewidths of the order of 40 nm. Below that linewidth, the diffusion rate increases rapidly relative to the deprotection rate, leading to complete image loss at about 25 nm linewidth. A similar analysis done for the TBI-T/PTBOCST resist system shows that diffusion begins to dominate blurring at a linewidth of 340 nm, and the lines are completely gone at 170nm. This is a consequence of the much higher mobility of TBI-T in the polymer.[3]

Although this type of examination of resist performance using the PEB model is appealing, it is not justifiable unless the reaction kinetics have been validated experimentally for 3-dimensional patterns printed at the design wavelength using realistic light doses and PEB conditions. In particular, our use of 193 nm exposure to generate very high acid concentrations may have caused us to access a different chemical regime than is active under normal imaging conditions in the 248-257 nm range. In this paper we describe experiments to measure directly the extent of deprotection in patterned images formed at 257 nm in PTBOCST-based resists, and compare them to predictions using our existing reaction-diffusion model. The results show that the 1-dimensional kinetics determined at 193 nm are valid for 3-dimensional imaging in these systems, and provide new insight to the process of latent image formation during PEB.

Experiment and Simulation

(a) Basic design of the experiment. In previous studies we measured coupled acidolysis-diffusion kinetics as a function of time by performing IR measurements on resist films as they deprotected on a hot stage.[2-4] This was made possible by using low PEB temperatures to slow the deprotection rate, and by using sufficiently high exposure doses that the PAG was completely decomposed in the top region of the resist, reducing the sensitivity of the kinetics to environmental contaminants such as amines during the long measurement times used.[13] This approach provides adequate detail for study of blurring in one dimension. In the present work we sought to characterize the extent of blurring in three dimensions. Ideally, such a study would involve full spatially resolved, nanometer scale chemical characterization of a resist film as a function of time, dose and pattern dimension. Although progress is being made,[14] this is beyond current techniques. We have taken an alternative approach. We use a large area probe (infrared spectroscopy, 100 μm spot) to provide chemical specificity, and compare blanket and line-space array patterned film compositions after PEB to gauge blur. A schematic is shown in Figure 2. The blanket-exposed regions provide an internal standard for the maximum extent of deprotection possible for a given set of conditions. A patterned region receiving the same dose will show somewhat less total reaction, depending on extent of blur. Detailed simulations carried out for each set of experimental conditions are directly compared to experiment both to assess the validity of the model, and to gain insight to the evolution of the printed image during processing.

(b) Materials. The materials used were the same as in previous work to minimize discrepancies due to variations in polymer or PAG batches.[2-4] 5-inch silicon wafers coated with 100 nm thick BARL anti-reflection layers were used as substrates. Formulations of PTBOCST with 0.045

mol/kg of solids of TBI-T or TBI-PFBS PAG, and PTBOCST/TBI-PFBS with 0.05 equivalents of TBAH prepared in propylene glycol methyl ether acetate solution were used. Resist films of approximately 1200 nm thickness were spin coated at 3000 rpm and post-apply baked at 130 C for 90 s. Film thicknesses were measured by optical reflectance (Nanospec).

PTBOCST resist is notoriously susceptible to airborne basic contaminants.[13] Species such as n-methyl pyrrolidone at the ppb level have been shown to penetrate the resist film rapidly even at room temperature, neutralizing photogenerated acid and inhibiting image formation. Resist copolymers, processing and film handling techniques have been developed to mitigate these problems in clean room settings. While our film preparation area has amine filters, the laboratory used for exposures and PEB have amine levels ranging from 3.5 to 15 ppb (average of 7 ppb) over a 48 hour period measured using an Extraction Systems TMB150 process monitor, with no apparent correlation between time of data or activities in the lab. As will be described in the results section, it appears that amine exposure has affected the accuracy of some of the data by systematically suppressing the deprotection reaction at various locations on some wafers.

(c) Exposures All illuminations were carried out using an interferometric lithography apparatus that has been described previously.[15] Briefly, 257 nm light is generated by intracavity doubling of an Ar ion laser. The beam is passed through a spatial filter to generate an ideal Gaussian, and split into 2 identical beams. The beams, s-polarized with respect to the wafer plane, recombine at the surface of a resist film, generating a grating with an elliptical footprint. The beam diameter used in this work was about 1 cm, with an 0.1 mm diameter region in the center that has nearly uniform intensity. The depth of field of the interference pattern is much larger than the resist film

thickness, ensuring that the light modulation was essentially 100% across the fringes through the entire film. The interferometer was equipped with 2 shutters allowing either single beam or dual beam illumination. This enabled printing of line-space array patterns and blanket-illuminated fields at the same dose side-by-side on the wafer. The interferometer was set for pitches of 192 nm and 866 nm in order to investigate large and small linewidths. Incident doses were 1, 2.75, 4.5, 6.25 and 8 mJ/cm^2.

(d) Process conditions. The wafers were post-expose baked in air on a CEE model 1000 hotplate for 1, 2, 5 or 10 minutes at 85 C. This procedure ensures that all wafers have a well-defined time-temperature history, and minimizes errors in the kinetics due to exposure of wafers to ambient contaminants after acid generation.

(e) Infrared spectroscopy. Infrared spectra were recorded at the center of each exposed ellipse and in a nearby unexposed region using a Nicolet Continuum infrared microscope attached to a Nicolet Nexus 470 Fourier transform infrared spectrometer. All spectra were obtained in reflectance mode. In previous work[2] the CO transition at 1760 cm^{-1} was used in transmission to measure extent of deprotection by normalizing time-dependent data to initial absorbance for each wafer. It was found in the present work that the scatter in the data was very large when this peak was used for a set of locations on a wafer, most likely due to variations in local thickness, composition and contamination level. Therefore, a pair of C-H stretch absorptions at 2981 cm^{-1} (assigned to the BOC protecting group) and 2927 cm^{-1} (assigned to the polymer backbone) were used to determine the PTBOCST amount.[16] A spectrum of the region is shown in Figure 3. Although the peaks are small compared to the CO transition from the protecting group used in

prior work,[2-4] they are close together in energy, and only the 2981 cm^{-1} peak changes appreciably in intensity with deprotection so the other acts as an internal standard when calibrated with materials of known composition. When the peak ratios are normalized to ratios obtained for unexposed regions on the wafer, quantitative and reproducible data are obtained despite substantial shifts in baseline position and slope, a consequence of variations in thin film interference as thickness changes during deprotection,[17] and the location of the CH_2 transitions on top of other absorptions at the edge of a very broad OH stretch from the hydroxystyrene (HOST) deprotection product. Reproducibility was assessed by printing redundant spots on each wafer, and by repeating runs for each set of conditions at least once for all but the PTBOCST/TBI-PFBS/TBAH system. Calibration points were obtained by taking authentic spectra of unexposed PTBOCST, a 60:40 copolymer of TBOCST and HOST, and a fully deprotected film, as shown in Figure 4. Use of a copolymer to represent partly deprotected materials is not ideal because there are likely to be substantial differences in composition between the two that are poorly understood.[18] Accordingly, conversion of the infrared data into quantitative composition data using this curve is a significant source of systematic error in this work. The error increases dramatically with extent of reaction because of increasing spectral complexity. We estimate the error to range from ± 5% at low doses and bake times to ±25% at high doses and bake times. We suspect the extent of reaction may be systematically underestimated using this approach, however reproducibility is within 5% for all data excepting a few cases where airborne base contamination is evident.

(e) Optical properties and calculation of the acid image. In order to predict the experimental results the precise absorbed light image in the resist was calculated using n and k measured by

reflectance at 257 nm for each layer.[19] Refractive index values were 1.6432-0.01372i (PTBOCST), 1.795-0.2602i (BARL) and 1.6432-3.9287i (silicon).[20] The absorbance and reflectance for the resist-BARL-silicon stack on each wafer were then calculated for the angles of incidence used for the 192 and 866 nm pitch illuminations[15] and the specific layer thicknesses. To provide initial acid images for input to the reaction-diffusion simulations, the aerial image for a single period in the interference pattern was modelled using a 15 column 5 row grid oriented transverse to the line. The light intensity is assumed to be constant along each line. A 2-dimensional map of local intensities at the center of the Gaussian laser beam was determined using the $\sin^2$ intensity pattern generated interferometrically, the actual resist film thickness, and the total absorbed dose for each pitch and incident dose. Similarly, a blanket illumination image was calculated for the same total incident dose. The use of BARL minimizes internal reflections in the resist films, simplifying the image considerably. The absorbed light intensity was converted into initial acid concentration distributions by using an experimentally determined value of 0.0603 for the acid yield per absorbed photon.[2,21]

(g) Simulations. The extent of deprotection was predicted for each set of experimental conditions using the VSIM simulation code and reaction-diffusion mechanisms and rate constants reported previously.[2,3] Briefly, the PEB process is modelled using the experimental acid latent image and full coupled reaction-diffusion kinetics. These include both thermal and acid-catalyzed deprotection steps and two diffusion paths describing migration of proton-anion pairs through nonpolar PTBOCST and its polar PHOST deprotection product. There are no adjustable parameters.

Results

Families of infrared spectra were obtained for blanket and interferometric exposures of the following resists: PTBOCST/TBI-PFBS at 192nm and 866 nm pitches, PTBOCST/TBI-T at 193nm and 866 nm pitches, and PTBOCST/TBI-PFBS/TBAH at 192 nm pitch. A typical set of curves is shown in Figure 5. PTBOCST fractions were extracted from the data as described in the experimental section.

Extents of reaction obtained from the infrared spectra as described in the experimental section are compared to simulations in Figures 6-10. As discussed in the introduction, significant blur was expected only for the TBI-T/PTBOCST resist system at small pitch, and indeed the blanket and IL exposures resulted in the same extent of reaction for that system (Figure 9). In the other four cases, the IL exposures showed less reaction than the blanket exposures, indicating that blur was significantly reduced. The overall degree of blur was greater for the small pitch exposures (96 nm lines and spaces) than the large pitch exposures (433 nm lines and spaces). Two complete data sets are shown for the TBI-PFBS/ PTBOCST system to illustrate the reproducibility of the data. In all cases the discrepancy between simulations and experiment is at most 30%.

The agreement between prediction and experiment can be assessed in two ways: by comparing the trends among the blanket/IL pairs for each set of reaction conditions, and by comparing the PTBOCST fractions directly. Although the simulations and the data are in excellent agreement by both measures overall, small systematic deviations in PTBOCST fractions are evident. It can be seen in the Figures that the 1 and 2.75 mJ/cm^2 PTBOCST fraction data always show less reaction than predicted, while the higher doses are in better agreement. We also find that one of

the 10 min PEB TBI-PFBS wafers (Figure 6) and the 5 and 10 min PEB TBI-PFBS/PTBOCST/base wafers (Figure 10) show less reaction at all doses. That the discrepancy between experiment and prediction always appears as an observation of reduced reaction suggests that adventitious base contamination is largely responsible. Further support for this interpretation is found in the trends in IL/blanket intensities. Simulations and experiment are in closest agreement when PTBOCST fractions match, and trends show the IL data are systematically too close to the blanket data when the fractions are too small. Since the presence of base serves to reduce the amount of acid available, the image contrast is reduced when base is present.

Discussion

The agreement between experiment and predictions for PTBOCST resists provides clear evidence that the PEB reaction-diffusion kinetics determined in a 1-dimensional geometry can be used to describe pattern formation in this system. There is no evidence that essential elements of the model are missing - e.g. anisotropic diffusion due to presence of the pattern, acid loss due to volatilization, or free volume effects - and therefore it can be considered to provide a reasonable description of PEB chemistry and physics. With this validation of the PEB model, the spatial distributions of acid and polymer predicted by the simulations can be used to visualize the IL/blanket exposure trends in the experimental data. Moreover, they provide insight to the connection between the initial acid latent image and the developable image it produces, and to the chemistry that contributes to blur.

Maps of acid and PTBOCST distributions for a single period in a line-space array printed in a 1200 nm thick film are presented in Figures 11-13 for the 8 mJ/cm^2 exposures, 1, 2 and 5 min bake times. It can be seen that for all resists the acid image spreads more at small pitch than at large pitch, consistent with the larger concentration gradients present. The diffusion rate of TBI-T is sufficiently high that at small pitch the initial acid latent image has essentially disappeared within the first minute at 193 nm pitch, in agreement with the model simulations described in the introduction. Close inspection of the PTBOCST maps reveals that although the ratio of developable linewidths (> 80% deprotection) to nominal linewidths is comparable for all five cases, there is considerable variation in image contrast as depicted by the gray scale. This coupling of reaction and diffusion manifested itself differently in our previous 1-D studies, which showed substantial spreading of the deprotected polymer profile beyond the acid profile.[2] This is a kinetic effect: in the 433 and 96 nm line-space array structures the acid gradients are much steeper and therefore the diffusion rates are faster, and the nominally unexposed areas can be populated with acid diffusing from two adjacent lines instead of a single layer. The resulting developable linewidths are relatively narrow because the acid at the edge of the lines and in the unexposed areas rapidly acquires a relatively uniform distribution causing slow isotropic deprotection, while the center of the line deprotects rapidly and retains its average acid concentration (see Figure 9, reference 2 for an illustration). This is to be expected because the deprotection product, HOST, accelerates the local thermal deprotection process while reducing the rate of acid diffusion and acid-catalyzed deprotection.[17,22]

The IL/blanket trends measured in the experiment and extracted from the simulations reflect *both* developable linewidth and contrast between levels of deprotection in exposed and nominally

unexposed areas. Since there is relatively little blur in the developable lines, this suggests that the role of development kinetics in partly deprotected regions of the polymer film may be as important as that of PEB kinetics and resist composition in determining blur. Indeed, the critical ionization model for resist dissolution connects the local dissolution rate to the local extent of deprotection,[23] and does not include a sharp solubility cutoff at 80% deprotection. We are currently using our simulated polymer latent images to investigate this aspect of image formation, and have found that the dissolution kinetics play a critical role in determining lineshape. More simplified dissolution models which simply transform the post-PEB latent image may have difficulty in predicting lineshapes correctly, particularly if the latent image is not realistic.

The approximate developable image profiles all have a V-shape. This is a consequence of the PEB temperature used. A series of simulations were carried out for the TBI-PFBS/ PTBOCST system at 100 C for the full 1 - 8 mJ/cm^2 dose range, and bake times of 1, 2 and 5 minutes (see Figure 14). The model predicts that the wall shape will vary significantly across this range, with more square profiles being found in the 6.25 - 8 mJ/cm^2 range.

There are numerous models for the PEB process that convert an aerial image into a developable image.[8,24-26] All are based on a simplified treatment of the thermal and acid-catalyzed deprotection chemistry, and typically require careful optimization of variable parameters to reproduce experimental data. Our PEB model, which is chemically and physically accurate, successfully reproduces experiments over a wide range of conditions and resist compositions with no adjustable parameters. Moreover, direct comparison with time-dependent measurements

is made possible by our use of a simulation method that provides an absolute time base. The insights gained by development and extension of this model should prove to be very useful for identification of molecular-level factors that control imaging below 100nm, and creation of improved simplified models for use on a more limited basis with popular lithography simulation packages.

Acknowledgmenrs

We thank Amy Lytle (APS/IBM Summer Fellowship for Women) for her measurements of the reflectances used in this work. We are grateful to Greg Wallraff, Hiroshi Ito, Carl Larson, Greg Breyta and Bob Allen for useful discussions during the course of this work, and to Dean Pearson for technical assistance.

References

1. G. M. Wallraff and W. D. Hinsberg, *Chem. Rev*. **99**, 1801 (1999).
2. F. A. Houle, W. D. Hinsberg, M. Morrison, M. I. Sanchez, G. Wallraff, C. Larson, and J. A. Hoffnagle, *J. Vac. Sci. Technol. B* **18**, 1874 (2000).
3. W. D. Hinsberg, F. A. Houle, M. I. Sanchez, M. E. Morrison, G. M. Wallraff, C. E. Larson, J. A. Hoffnagle, P. J. Brock, and G. Breyta, *Proc. SPIE, Advances in Resist Technology and Processing XVII*, **3999**, 148 (2000).
4. F. A. Houle, W. D. Hinsberg and M. I. Sanchez, unpublished work.
5. W. D. Hinsberg, F. A. Houle, G. M. Poliskie, D. Pearson, M. I. Sanchez, H. Ito, J. A. Hoffnagle, and M. Morrison, preliminary report in *Proceedings of the 12th International Conference on Photopolymers*, Society of Plastics Engineers, 249 (2001), full manuscript in preparation.
6. S. V. Postnikov, M. D. Stewart, H. V. Tran, M. A. Nierode, D. Medeiros and T. Cao, J. Byers, S. E. Webber and C. G. Willson, *J. Vac. Sci. Technol. B* **17**, 3335 (1999).
7. E. Croffie, M. Cheng and A. Neureuther, *J. Vac. Sci. Technol. B* **17**, 3339 (1999).
8. G. M. Schmid, V. K. Singh, L. W. Flanagin, M. D. Stewart, S. D. Burns and C. G. Willson, *Proc. SPIE, Advances in Resist Technology and Processing XVII*, **3999**, 675 (2000).
9. G. M. Schmid, M. D. Smith, C. A. Mack, V. K. Singh, S. D. Burns and C. G. Willson, *Proc. SPIE, Advances in Resist Technology and Processing XVIII*, **4345**, 1037 (2001).
10. S. D. Burns, M. D. Stewart, J. N. Hilfiker, R. A. Synowicki, G. M. Schmid, C. Brodsky and C. G. Willson, *Proceedings of the 12th International Conference on Photopolymers*, Society of Plastics Engineers, 323 (2001).

11. G. M. Wallraff, S. Bangsaruntip, N. Fender, W. Hinsberg, P. Brock, J. Hoffnagle, M. Sanchez, C. E. Larson, G. Breyta, W. Chau, *Proceedings of the 12th International Conference on Photopolymers*, Society of Plastics Engineers, 375 (2001).
12. H. Ito, *J. Photopolym. Sci. Technol*. **11**, 379 (1998).
13. W. Hinsberg, S. MacDonald, N. Clecak, C. Snyder and H. Ito, *Proc. SPIE, Advances in Resist Technology and Processing X*, **1925**, 43 (1993).
14. B. Dragnea, J. Preusser, J. M. Szarko, S. R. Leone and W. D. Hinsberg, J. *Vac. Sci. Technol. B* **19**, 142 (2001).
15. W. D. Hinsberg, F. A. Houle, J. Hoffnagle, M. Sanchez, G. Wallraff, M. Morrison and S. Frank, *J. Vac. Sci. Technol. B* **16**, 3689 (1998).
16. D. Dolphin and A. WIck, "Tabulation of Infrared Spectral Data", Wiley-Interscience, New York, 1977, Chapter 1.
17. G. Wallraff, J. Hutchinson, W. Hinsberg, F. A. Houle, P. Seidel, R. Johnson, and W. Oldham, *J. Vac. Sci. Technol. B* **12**, 3857 (1994).
18. H. Ito and M. Sherwood, *Proc. SPIE, Advances in Resist Technology and Processing XIV*, **3678**, 104 (1997).
19. H. A. Macleod, *Thin-film optical filters*, McGraw-Hill, 1989.
20. J. Rogers, IBM Burlington, unpublished data.
21. D. McKean, O. Schaedeli and S. MacDonald, J. Polymeer Sci. Part A: Polymer Chem., 27, 3927 (1989).
22. H. Ito, J. Polym. Sci. A **24**, 2971 (1986).
23. L. W. Flanagin, C. L. McAdams, W. D. Hinsberg, I. C. Sanchez and C. G. Willson, *Macromolecules* **32**, 5337 (1999).

24. A. A. Krasnaperova, M. Khan, S. Rhyner, J. W. Taylor,Y. Zhu and F. Cerrina, *J. Vac. Sci. Technol. B* **12**, 3900 (1994); L. Capodeici, A. Krasnaperova, F. Cerrina, C. Lyons, C. Spense and K. Early, *J. Vac. Sci. Technol. B* **13**, 2963 (1995).

25. J. S. Peterson, C. A. Mack, J. M. Thackeray, R. Sinta, T. H. Fedynyshyn, J. M. Mori, J. D. Byers and D. A. Miller, *Proc. SPIE, Advances in Resist Technology and Processing XII*, **2438**, 153 (1995), A. Sekiguchi, C. A. Mack, M. Isono and T. Matsuzawa, *Proc. SPIE, Advances in Resist Technology and Processing XVI*, **3678**, 985 (1999).

26. E. Croffie, L. Yuan, M. Cheng and A. Neureuther, *Proc. SPIE, Advances in Resist Technology and Processing XVIII*, **4345**, 983 (2001).

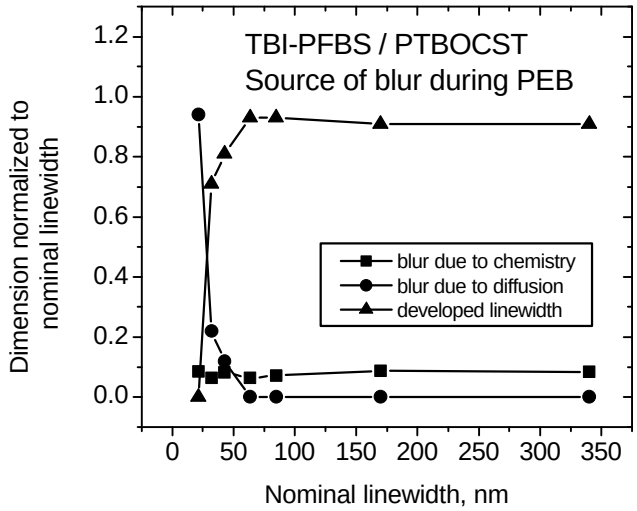

Figure 1. Chemical and diffusive contributions to blur predicted for TBI-PFBS/PTBOCST resist, 2 mJ absorbed dose, PEB at 100C for 2 min for pitches ranging from 680 nm to 42.6 nm. Chemical contributions were estimated by calculating developable linewidths with the diffusion coefficient set to 0. The diffusive contributions were estimated by subtracting chemical contributions from developable linewidths calculted with a full reaction-diffusion model.

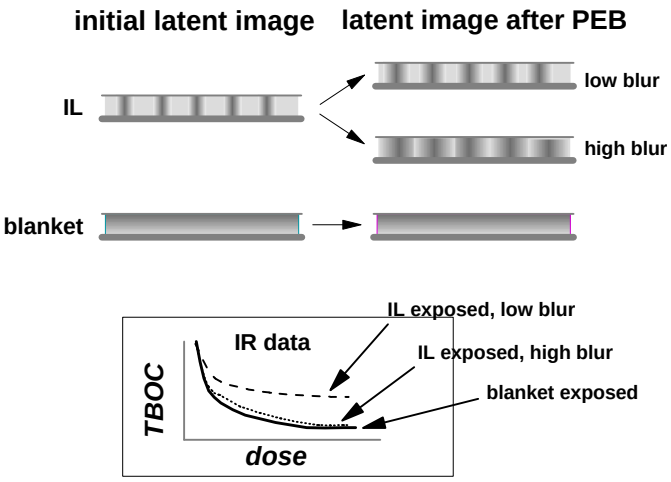

Figure 2. Diagram of blurring experiment design. IL and blanket exposures at constant dose are made side-by-side and the extent of deprotection in each is compared by infrared spectroscopy. The blanket exposures provide a measure of minimum image definition, or maximum blur.

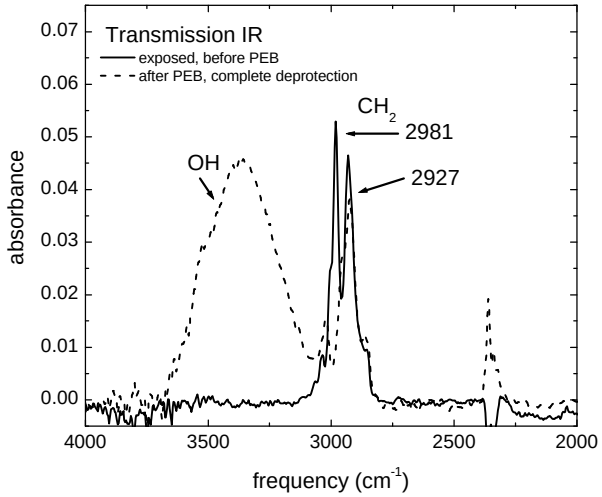

Figure 3. IR data for protected (solid line) and fully deprotected (dashed line) PTBOCST showing detail of the CH_2 region used to measure resist composition in this work.

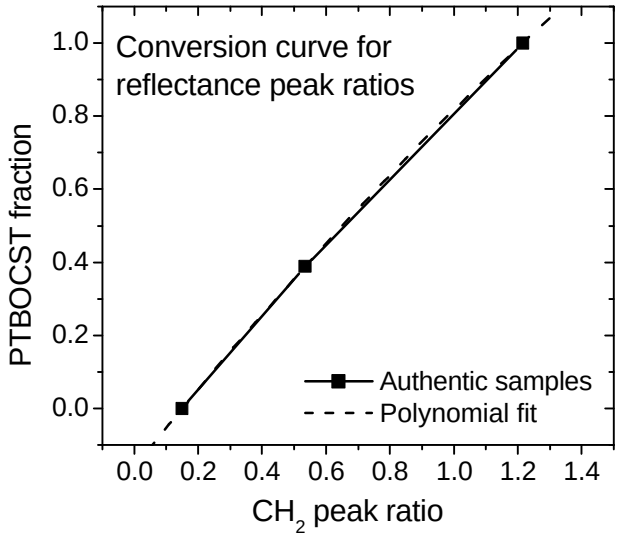

Figure 4. Calibration curve to convert CH_2 peak ratios to PTBOCST compositions.

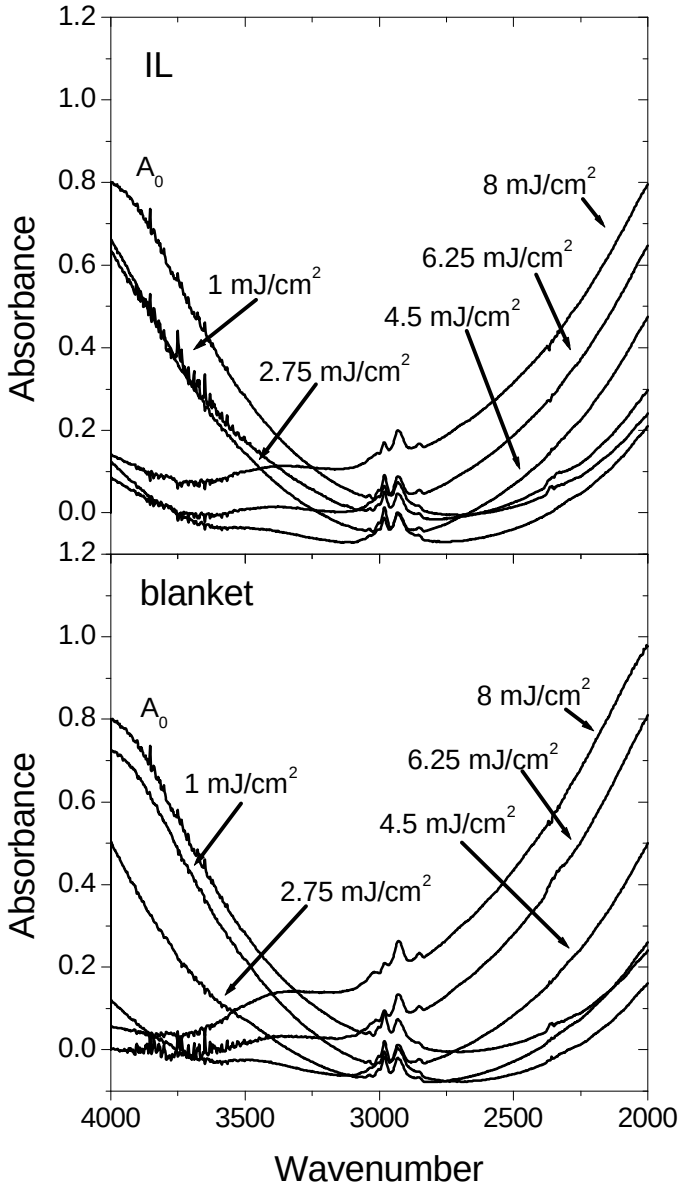

Figure 5. Typical IR reflectance curves for a range of doses, 10 min bake time. The spectrum for an unexposed region (A_0) is also shown.

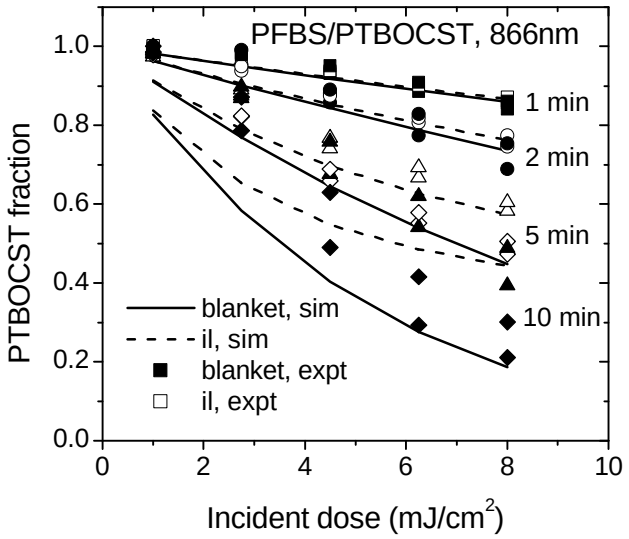

Figure 6. Experiment and simulations for TBI-PFBS/PTBOCST resist as a function of PEB time and dose, 866 nm pitch. Two sets of experimental data for each bake time - □1 min, ∘2 min, △5 min, ◇10 min- are shown.

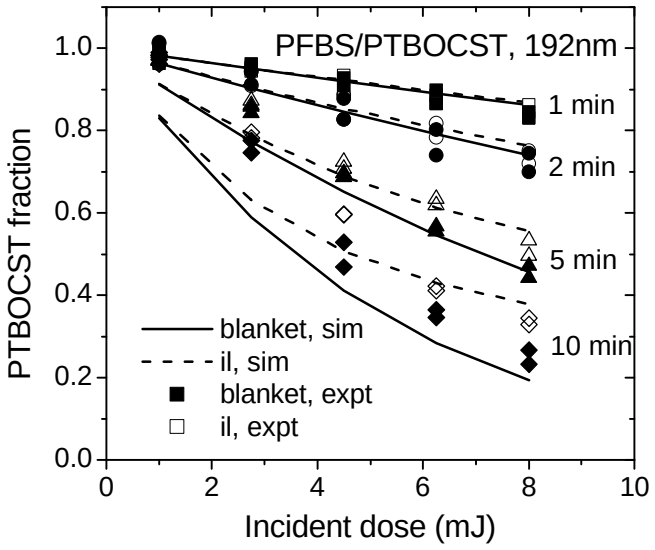

Figure 7. Experiment and simulations for TBI-PFBS/PTBOCST resist as a function of PEB time and dose, 192 nm pitch, 85C. Two sets of experimental data for each bake time - □1 min, ◦2 min, △5 min, ◇10 min- are shown.

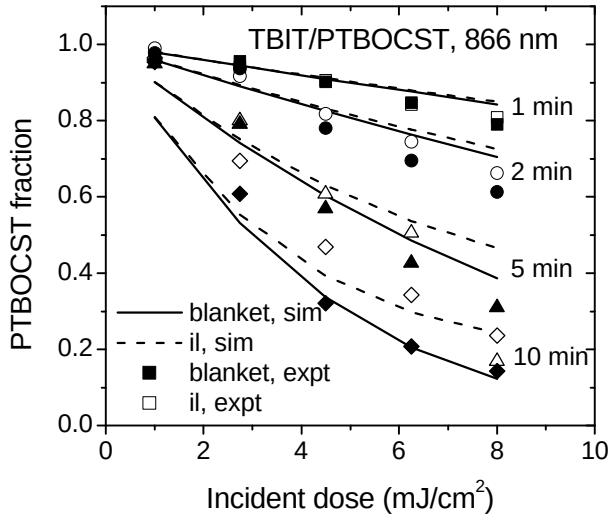

Figure 8. Experiment and simulations for TBI-T/PTBOCST resist as a function of PEB time and dose, 866 nm pitch, 85C. Bake times of -□1 min, ◦2 min, △5 min, ◇10 minare shown.

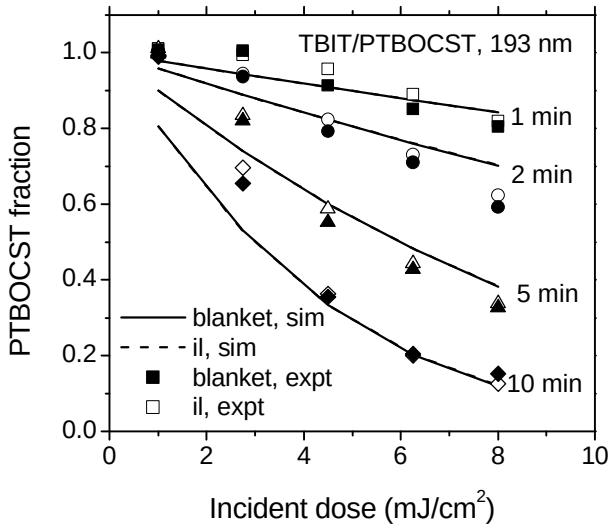

Figure 9. Experiment and simulations for TBI-T/PTBOCST resist as a function of PEB time and dose, 193 nm pitch, 85C. Bake times of -□1 min, ◦2 min, △5 min, ◇10 minare shown.

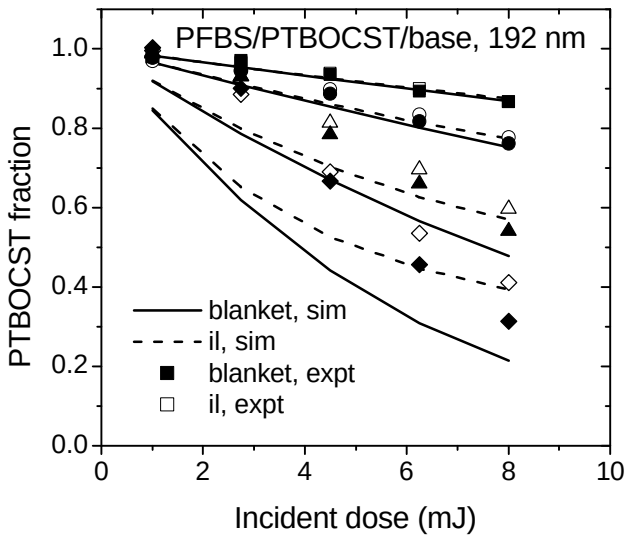

Figure 10. Experiment and simulations for TBI-PFBS/PTBOCST/0.05eq TBAH resist as a function of PEB time and dose, 192 nm pitch, 85C. Bake times of □1 min, ◦2 min, △5 min, ◇10 min are shown.

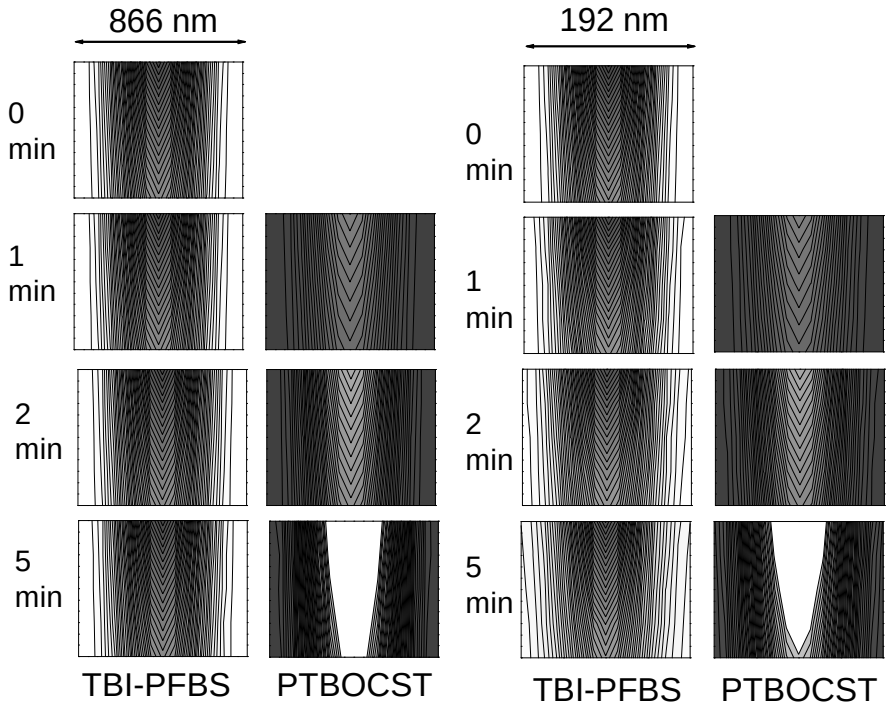

Figure 11. Latent images of acid (TBI-PFBS) and deprotected polymer (PTBOCST) for a single period of a 866 nm and a 192 nm line-space array in a 1200 nm thick TBI-PFBS/PTBOCST resist film, 8 mJ/cm^2 incident dose, evolving as a function of time during an 85 C PEB. The grey scale ranges from 0 (white) to 1.8e-20 moles (black) for the acid latent image, and from 100% protected (black) to 20% or less protected (white) for the polymer latent image. The resulting white regions approximate the developable image. Despite the more extensive blurring of the 192 nm pitch image, the developable images at the two pitches are comparable except near the bottom of the film, where the drop in acid concentration in the 192 nm pitch-exposed material has resulted in a noticeably slower overall deprotection rate.

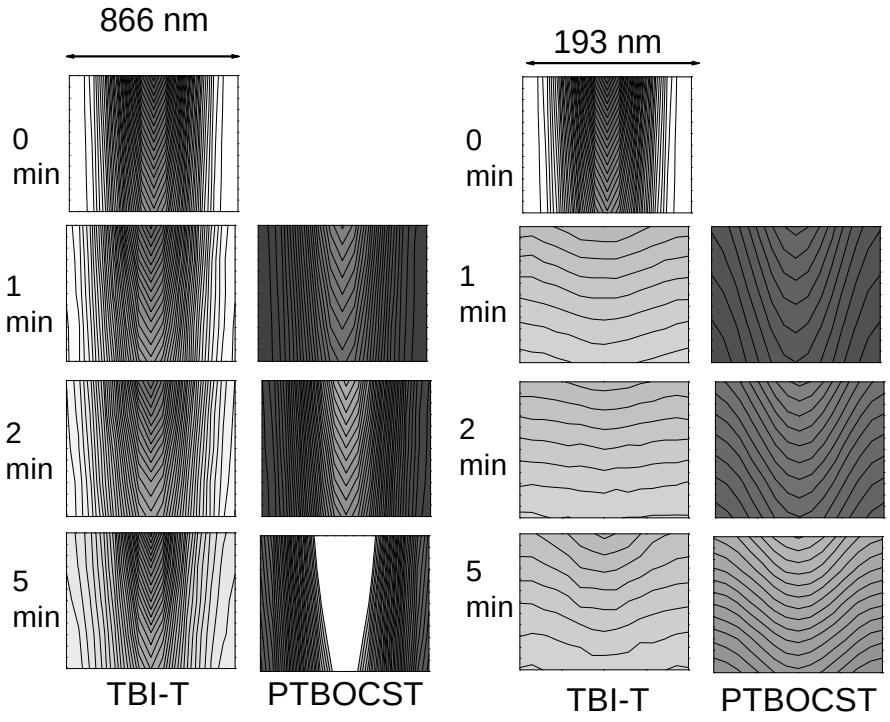

Figure 12. Latent images of acid (TBI-T) and deprotected polymer (PTBOCST) for a single period of a 866 nm and a 193 nm line-space array in a 1200 nm thick TBI-T/PTBOCST resist film, 8 mJ/cm^2 incident dose, evolving as a function of time during an 85 C PEB. The grey scales are the same as in Figure 11. Blurring is extensive for both pitches. The 193 nm latent image has completely disappeared within the first minute, and only the 866 nm lines are actually printed. Although the linewidths are about the same as for the TBI-PFBS system at 866 nm, the contrast of the developable image in TBI-T/PTBOCST is much lower.

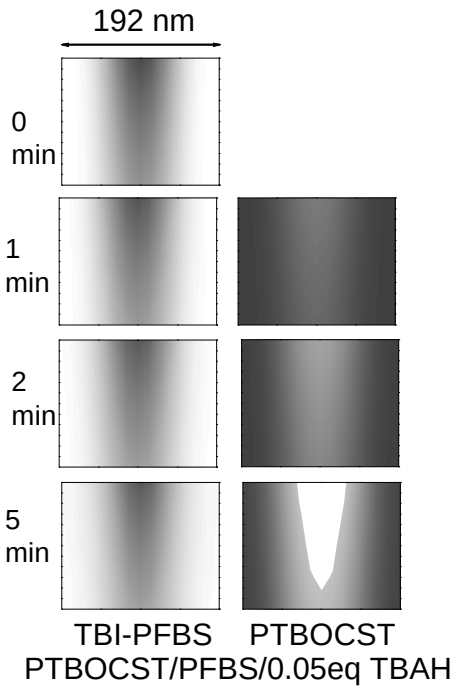

Figure 13. Latent images of acid (TBI-PFBS) and deprotected polymer (PTBOCST) for a single period of a 192 nm line-space array in a 1200 nm thick TBI-PFBS/PTBOCST/0.05eq TBAH resist film, 8 mJ/cm^2 incident dose, evolving as a function of time during an 85 C PEB. The grey scales are the same as in Figure 11. Although blurring is not significantly reduced compared to the base-free resist, the developable image is narrower and shallower because the overall acid concentration is proportionately lower.

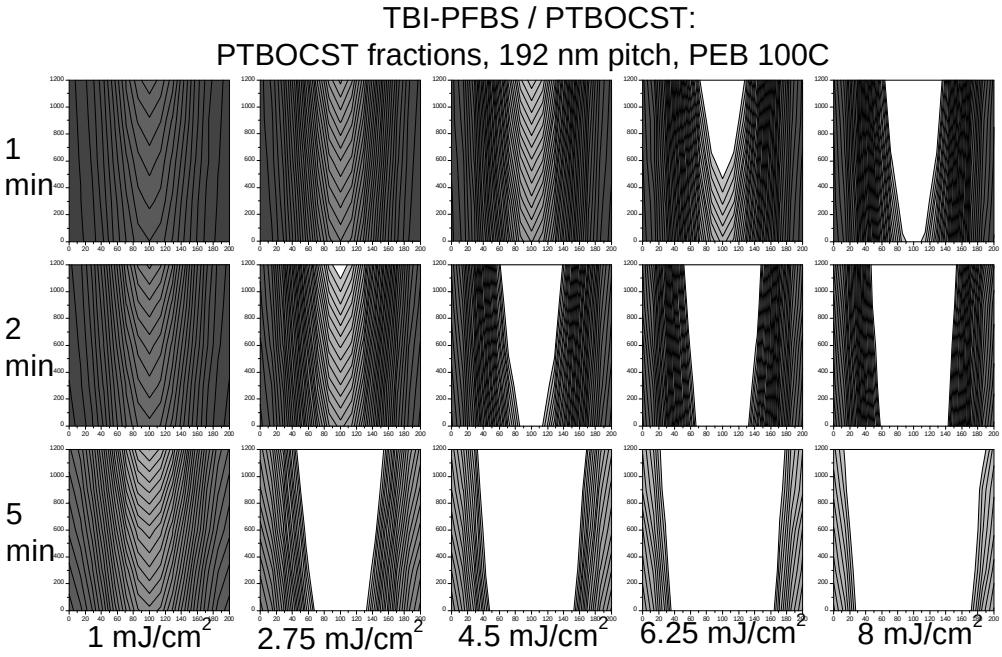

Figure 14. Predicted developable polymer latent images for 1.2 mm-thick films of TBI-PFBS/PTBOCST resist as a function of PEB time and dose, 85C. The gray scale is the same as in Figure 11.